Loss of C-5 sterol desaturase activity results in increased resistance to azole and echinocandin antifungals in a clinical isolate of *Candida parapsilosis*

Jeffrey M. Rybak [a], C. Michael Dickens [b], Josie E. Parker [c], Kelly Caudle [d], Kayihura Manigaba [a], Sarah G. Whaley [a], Andrew Nishimoto [a], Arturo Luna-Tapia [a], Sujoy Roy [e], Qing Zhang [a], Katherine S. Barker [a], Glen E. Palmer [a], Thomas R. Sutter [b], Ramin Homayouni [e], Nathan P. Wiederhold [f], Steven L. Kelly [c], and P. David Rogers [a,†]

[a] Department of Clinical Pharmacy, College of Pharmacy, University of Tennessee Health Science Center, Memphis, Tennessee, USA

[b] W. Harry Feinstone Center for Genomic Research, University of Memphis, Memphis, Tennessee, USA

[c] Institute of Life Science, Swansea University Medical School, Swansea, Wales, United Kingdom

[d] Department of Pharmaceutical Sciences, St. Jude Research Hospital, Memphis, Tennessee, USA

[e] Bioinformatics Program, University of Memphis, Memphis, Tennessee, USA

[f] Fungus Testing Laboratory, University of Texas Health Science Center San Antonio, San Antonio, Texas, USA

[†] Address correspondence to P. David Rogers, Email: progers3@uthsc.edu

Running title: *ERG3*-mediated multidrug resistance in *Candida parapsilosis*

Correspondent footnote: P. David Rogers

Department of Clinical Pharmacy

University of Tennessee Health Science Center

881 Madison Ave., Room 338

Memphis, TN 38163

Tel: 901-448-7217

Fax: 901-448-1741

Email: progers3@uthsc.edu

Abstract word count: 249

Total word count: 4,098

Abstract (249 words out of 250 words max)

Among emerging non-*albicans Candida* species, *C. parapsilosis* is of particular concern as a cause of nosocomial bloodstream infections in neonatal and intensive care unit patients. While fluconazole and echinocandins are considered effective treatment of such infections, recent reports of fluconazole and echinocandin resistance in *C. parapsilosis* indicate a growing problem. The present study describes a novel mechanism of antifungal resistance in this organism affecting the susceptibility of azole and echinocandin antifungals in a clinical isolate obtained from a patient with prosthetic valve endocarditis. Transcriptome analysis indicated differential expression of several genes in the resistant isolate including upregulation of ergosterol biosynthesis pathway genes *ERG2*, *ERG5, ERG6*, *ERG11, ERG24*, *ERG25,* and *UPC2*. Whole-genome sequencing revealed the resistant isolate possessed an *ERG3* mutation resulting in a G111R amino acid substitution. Sterol profiles indicated a reduction in sterol desaturase activity as a result of this mutation. Replacement of both mutant alleles in the resistant isolate with the susceptible isolate's allele restored wild-type susceptibility to all azoles and echinocandins tested. Disruption of *ERG3* in the susceptible and resistant isolates resulted in a loss of sterol desaturase activity, high-level azole resistance, and an echinocandin-intermediate to -resistant phenotype. While disruption of *ERG3* in *C. albicans* resulted in azole resistance, echinocandin MICs, while elevated, remained within the susceptible range. This work demonstrates that the G111R substitution in Erg3 is wholly responsible for the altered azole and echinocandin susceptibilities observed in this *C. parapsilosis* isolate and is the first report of an *ERG3* mutation influencing susceptibility to the echinocandins.

Introduction

Candida species are among the most common causes of bloodstream infections in the United States and are associated with high morbidity and mortality. While *C. albicans* is the most commonly isolated causative agent of candidemia, infections due to other non-*albicans* species of *Candida* have been increasing in recent decades (1-3). Of these, *Candida parapsilosis* is of particular concern as a human fungal pathogen. It exhibits a wide growth capacity on surfaces, such as prosthetic materials and intravascular devices and grows well within parenteral nutrition. It persists in hospital environments and may be transmitted nosocomially via hand carriage. Low weight neonates and intensive care patients are among the highest at risk for infections with *C. parapsilosis* (4). Relative to what is known in *C. albicans*, there is little information regarding the mechanisms by which antifungal drug resistance develops in *C. parapsilosis*. Uniquely among *Candida* species, *C. parapsilosis* demonstrates intrinsic reduced in vitro susceptibility to the echinocandins, presumably as a result of a naturally-occurring polymorphism in *FKS1* (5). While uncommon, clinical resistance to this class of antifungals has emerged in *C. parapsilosis* (6, 7). Azole resistance, on the other hand, is more common in *C. parapsilosis*, with rates of fluconazole resistance being approximately five times that of *C. albicans* (8). Recent reports indicate that overexpression of the drug efflux pump Mdr1 as well as an increase in, or mutation of, the target of the azoles, Erg11, contributes to azole resistance in this species (9-12).

In this study, we investigated the mechanisms underlying antifungal drug resistance in a clinical isolate of *C. parapsilosis* by comparing it to a genetically-matched, antifungal-susceptible isolate from the same patient. Through whole

transcriptome and genome sequence analysis and allelic replacement, we demonstrate that a mutation in *ERG3* leads to resistance to the azole antifungals via alternate sterol production. Additionally, we discover that this mutation in *ERG3*, as well as its disruption, also causes increased resistance to the echinocandins. This is the first report of an *ERG3*-related resistance mechanism in *C. parapsilosis* and is the first evidence in any *Candida* species that such mutations also influence susceptibility to the echinocandins.

Results

Clinical Isolates and Susceptibility Testing

The *C. parapsilosis* isolates used in this study were collected over the course of multiple hospitalizations from a patient with aortic valve endocarditis, as outlined elsewhere (13). These isolates were kindly provided by Dr. Jose Vazquez. The originally reported antifungal susceptibilities (using the previous CLSI M27-A2 recommended methodologies) for both the susceptible isolate collected at initial admission (Isolate 1) as well as for the subsequently collected resistant isolate (Isolate 2) for several azoles, echinocandins, and amphotericin B are shown in Tables 3A and 3B. MIC (minimum inhibitory concentration) values for fluconazole, itraconazole, voriconazole, posaconazole, caspofungin, anidulafungin, micafungin, and amphotericin B were independently determined for this study by the Fungus Testing Laboratory at the University of Texas Health Sciences Center at San Antonio (Tables 3A and 3B). Isolate 1 was susceptible to all azoles tested when read at both 24 and 48 hours, and likewise

to amphotericin B and all echinocandins tested (determined at 24 hours). Interestingly, when determined at 24 hours, Isolate 2 appeared susceptible to all azoles tested, whereas when determined at 48 hours, was resistant to all azoles tested. These results were consistent upon repeat testing. Isolate 2 also exhibited an increase in MIC for the echinocandins, reaching the intermediate range for micafungin and anidulafungin. No change in susceptibility to amphotericin B was observed. In separate experiments, 24 and 48 hours growth curves were plotted for fluconazole MIC cultures (Figure 1). At both timepoints Isolate 2 phenocopied the *erg*3Δ/*erg3*Δ mutants.

Transcriptional Profiling Reveals Increased Expression of Ergosterol Biosynthesis Genes

Global changes in gene expression between Isolates 1 and 2 were determined by RNA sequencing. A total of 378 genes (Table S1) were observed to be reproducibly upregulated by a minimum of 1.5-fold in the resistant isolate as compared to the susceptible isolate. Of note, only three of these genes (*UPC2, ATC1*, and CPAR2_400860) have been characterized in *C. parapsilosis* at this time. Gene Ontology term analysis performed using the Candida Genome Database (www.candidagenome.org) revealed genes of the sterol metabolic process to be the most significantly enriched among all upregulated genes (p=2.96e^{-5}). Of these 14 genes, as shown in Table 4, the sterol regulatory transcription factor *UPC2* and the *C. parapsilosis* orthologs of identified CaUpc2 target genes (*ERG1, ERG2, ERG5, ERG6, ERG11, ERG24,* and *ERG25*) are included (14). Differential expression of key ergosterol biosynthesis genes, as well as the lack of a change in expression of the

multidrug transporter genes *CDR1*, *CDR2*, and *MDR1*, were confirmed with qRT-PCR (data not shown). An additional 32 genes were observed to be upregulated in the resistant isolate, but the extent of which could not be reliably quantified due to extremely low transcript counts in the susceptible isolate (Table S2). Genes which are reproducibly downregulated in the resistant isolate as compared to the susceptible isolate are listed in Table S3.

Next Generation Sequencing Identifies a SNP in ERG3 *in the Resistant Isolate*

To further characterize this matched isolate pair, whole genome sequencing was used to identify single nucleotide polymorphisms occurring in Isolate 2 as compared to Isolate 1 (Figure 2). There was a total of 462 SNPs detected, involving 305 individual genes. Many of the genes containing SNPs are involved in cell adhesion, biofilm formation, and cytoskeletal rearrangement. A homozygous nonsynonymous mutation was detected in *ERG3*, substituting a glycine to an arginine at position 111. This polymorphism was confirmed by Sanger-based sequencing (data not shown).

Analysis of Copy Number Variation and Loss of Heterozygosity

The Yeast Mapping Analysis Pipeline (Ymap; lovelace.cs.umn.edu/Ymap) was used to identify chromosomal copy number variation (CNV) and loss of heterozygosity (LOH) between Isolate 1 and Isolate 2 (15). CNV and SNP analysis of Isolate 1 revealed no segmental or chromosomal CNV, and scattered regions of increased heterozygosity across each chromosome (Figure 3A). Using the Isolate 1 analysis as a

parental reference isolate, the WGS data for Isolate 2 was then assessed. Unlike its parent isolate, Isolate 2 exhibited segmental tetraploidy in a single chromosome (Contig005809). In this region, containing 113 genes (Table S4), complete duplication across approximately 233,000 bases was observed (Figure 3B). Additionally, LOH analysis revealed that while relatively little allelic variation was present in Isolate 1, much of this variation has been lost in Isolate 2 (Figure S1).

Loss of Erg3 Activity Confers Increased Resistance to Echinocandins in C. parapsilosis *and to a Lesser Extent* C. albicans

We first deleted both alleles of *ERG3* in both the susceptible (Isolate 1) and resistant (Isolate 2) isolates. As expected, loss of *ERG3* resulted in resistance to all azoles tested (Table 3A). Surprisingly, deletion of *ERG3* also resulted in MICs that fell within the intermediate to resistant range for the echinocandins (Table 3B). In order to determine if this also occurs in the related species *C. albicans*, we tested the echinocandin susceptibilities of two independent *ERG3* deletion mutants constructed in two different backgrounds. In both cases deletion of *ERG3* resulted in negligible increases in echinocandin MICs (Table 3B).

The G111R Substitution in Erg3 Confers Reduced Susceptibility to Azoles and Echinocandins

In order to directly assess the role of the G111R amino acid substitution in Erg3 in the reduced susceptibility to azoles and echinocandins, we introduced the wild-type

171 *ERG3* alleles from the susceptible isolate (Isolate 1) into its resistant counterpart
172 (Isolate 2), creating a homozygous mutant, and performed susceptibility testing against
173 azoles and echinocandins. Introduction of the wild-type *ERG3* alleles to Isolate 2
174 restored susceptibility to all azoles tested (Tables 3A and 3B). Surprisingly,
175 susceptibility to the echinocandins was also restored to the levels observed in Isolate 1.

176

177 *The G111R Substitution in Erg3 Leads to Alterations in Sterol Biosynthesis*

178 As the mutation in *ERG3* is not a nonsense mutation, we questioned if,
179 alternatively, the activity of Erg3 is reduced by this mutation, leading instead to a less
180 functional protein. Perturbations in this protein would be evident with increases in
181 accumulated ergosta-7,22-dienol, episterol, and ergosta 7-enol. Sterol profiles were
182 obtained using GC/MS and are shown in Table 5. Isolate 1 exhibits a reasonably
183 normal sterol profile in which ergosterol comprised the highest percentage. On the
184 other hand, Isolate 2 exhibits profiles in which ergosta-7-enol and ergosta-7,22-dienol
185 represented the largest portion of the total cell fraction. This is consistent with a
186 reduction in sterol desaturase activity. Upon replacement of the mutant *ERG3* alleles in
187 Isolate 2 with the wild-type allele from Isolate 1, normal sterol profiles were restored.
188 Deletion of *ERG3* in both Isolate 1 (susceptible isolate) and Isolate 2 (resistant isolate)
189 resulted in profiles consistent with complete loss of Erg3 activity.

190

191 **Discussion**

192 Most of what is known about the genetic basis of antifungal resistance has been
193 determined from *C. albicans*. Mechanisms of azole resistance in this species include
194 overexpression of the gene encoding the target enzyme, Erg11, and nonsynonymous
195 mutations in both *ERG11* and *ERG3*. Additionally, upregulation of drug efflux pumps
196 represents an additional mechanism of azole resistance; ABC transporters Cdr1 and
197 Cdr2 confer resistance to multiple azoles, while the MFS transporter Mdr1 confers
198 resistance to fluconazole, ketoconazole, and voriconazole (16). Echinocandins, on the
199 other hand, function by inhibiting β-D-glucan synthase activity, encoded by *FKS1* in *C.*
200 *albicans* and *FKS1* and *FKS2* in *S. cerevisiae* (17). Although mutations within *FKS*
201 genes have been linked to echinocandin resistance in several species of *Candida* (18),
202 there are also additional mechanisms by which this resistance may occur. These
203 include the activation of signaling pathways which regulate stress response and PKC
204 cell wall integrity, as well as synthesis of ancillary cell wall components such as chitin
205 and mannan (19).

206 In the present study, RNA sequencing revealed the genes that are differentially
207 expressed between these two genetically-related clinical isolates. We did not observe
208 overexpression of any gene encoding a characterized multidrug transporter suggesting
209 that azole resistance was unlikely due to reduced intracellular accumulation of drug.
210 Furthermore, the observed 1.6 to 2.6- fold increased expression of *ERG11* in the
211 resistant isolate, as compared to the susceptible isolate, would alone not be expected to
212 produce high-level pan-azole resistance particularly in the absence of an accompanying
213 *ERG11* mutation. Lastly, we did not observe any change in gene expression that would

indicate a root cause for the observed reduction in echinocandin susceptibility, such as an increase in glucan synthase or chitin synthase expression.

Notably among the upregulated genes are several involved in the ergosterol biosynthesis pathway. This biosynthetic pathway results in the production of an essential fungal membrane component, ergosterol, and inhibition of the azole target sterol demethylase leads to production of toxic sterol intermediates (20). The azoles exploit this and function specifically by inhibiting the enzyme 14α- lanosterol demethylase, encoded by *ERG11*, leaving the cell unable to produce ergosterol (21). The genes which were observed to be upregulated within the resistant isolate, *ERG1, ERG2*, *ERG5, ERG6*, *ERG11, ERG24*, *ERG25, ERG27,* and *DAP1,* encode various proteins involved in sterol processing within this pathway and are located both upstream and downstream of the azole target, Erg11. Additionally, the gene encoding the sterol regulatory transcription factor Upc2 was upregulated. These observations are consistent with loss of sterol desaturase activity leading to decreased membrane ergosterol and activation of Upc2. In this way, an upregulation of these critical genes represents a response to facilitate increased conversion of lanosterol to ergosterol in the event that production had declined or been disrupted. This is further supported by the results of the whole genome sequencing of the isolate pair. Among a relatively small number of SNPs detected in the resistant isolate which do not occur in the susceptible isolate, a nonsynonymous mutation was identified in *ERG3*. This gene is located downstream in the ergosterol biosynthesis pathway relative to the genes found to be upregulated by RNA sequencing. The amino acid substitution, at position 111 of the predicted protein, changes a glycine to an arginine.

Mutation within *ERG3* has been documented in clinical isolates as well as passage-derived isolates of *C. albicans* and linked to both amphotericin B resistance and high-level azole resistance (22, 23). When azoles inhibit the function of 14α-demethylase and therefore the production of ergosterol, *ERG3* encodes an enzyme which converts the nontoxic 14α-methylated sterol intermediates into the toxic sterol 14α-methyl-ergosta-8,24 (28)-dien-3,6-diol. A reduction in or loss of this enzyme results instead in the accumulation of nontoxic ergosta-7,22-dienol. This leads to high levels of resistance to the azole drug class.

The loss of ergosterol in the yeast cell membrane, the target of amphotericin B, has been reported to result in resistance to this antifungal (24-26). However, using standard CLSI methods, we did not observe a reproducible increase in amphotericin B MIC at 24 or 48 hours for the *C. parapsilosis* or *C. albicans* mutants deleted for *ERG3* or for the *C. parapsilosis* mutant expressing the G111R mutation. The majority of *ERG3* mutations reported in the literature result in premature stop codons; however, there have been cases in which the strains instead exhibit nonsynonymous mutations, as observed in this isolate pair (22, 27-29).

The finding that the G111R amino acid substitution also explained the reduced susceptibility to the echinicandins observed in this isolate was unexpected as, until now, alterations in sterol desaturase activity have not been associated with this phenotype. It is important to note that deletion of *ERG3* had a similar effect on echinocandin susceptibility in *C. parapsilosis*, but this was not the case when *ERG3* was deleted in *C. albicans*. It is possible that a mutation in *ERG3* that impairs sterol desaturase activity,

combined with the naturally-occurring polymorphism in *FKS1* in *C. parapsilosis*, uniquely impacts echinocandin susceptibility in this *Candida* species.

Our finding of an *ERG3* mutation as a cause of azole resistance in this clinical isolate is supported by the recent work of Branco et al (30). In this study, a *C. parapsilosis* strain that was evolved to become resistant to posaconazole in the laboratory was found to have a similar (R135I) mutation in *ERG3* resulting in resistance to fluconazole, voriconazole, and posaconazole. Echinocandin susceptibilities however were not reported.

This matched isolate pair provided an opportunity to evaluate factors contributing to a unique case of antifungal resistance. We reasoned that the mechanism(s) underlying this resistance would be detectable among differences in gene expression and/or whole genome sequence analysis. Here we have demonstrated that a mutation in *ERG3*, which encodes a key enzyme for the production of the membrane sterol ergosterol, increases resistance to not only the azoles but also to the echinocandins in a clinical isolate. This is the first report of a mutation in *ERG3* influencing the susceptibility to the echinocandins and of a single mechanism that affects susceptibility to these two important classes of antifungals.

Materials and Methods

Strains and media. All *C. parapsilosis* isolates used in this study are listed in Table 1. Isolates were kept as frozen stock in 40% glycerol at −80°C and subcultured on YPD (1% yeast extract, 2% peptone, and 1% dextrose) agar plates at 30°C. YPD

liquid medium was used for routine growth of strains, while YPM (1% yeast extract, 2% peptone, 1% maltose) liquid medium was used for induction of the *MAL2* promoter in constructed strains. Nourseothricin (200 µg/ml) was added to YPD agar plates for selection of isolates containing the *SAT1*-flipper cassette (31). One Shot *Escherichia coli* TOP10 chemically competent cells (Invitrogen) were used for plasmid construction. These strains were grown in Luria-Bertani (LB) broth or on LB agar plates supplemented with 100 µg/ml ampicillin (Sigma) or 50 µg/ml kanamycin (Fisher Bioreagents), when needed.

Drug Susceptibility Testing. Susceptibility testing was performed by broth microdilution according to the methods in the CLSI M27-A3 reference standard (32). Testing was performed in at least duplicate for each isolate and each antifungal agent. The starting inoculum was between 0.5 – 2.5x10^3 cells /ml, and all testing was performed in RPMI 1640 with 0.2% glucose, buffered with 0.165M MOPS and adjusted to pH 7.0. Plates were incubated at 35°C, and MICs were read visually for the echinocandins and azoles at the lowest concentration that resulted in 50% growth inhibition compared to the drug free growth control at both 24 and 48 hours. For amphotericin B, the MIC was read as complete inhibition of growth at each of these time points.

The susceptibility results for fluconazole were also repeated and verified by broth microdilution using a microplate spectrophotometer with optical density readings as the endpoint. Each strain was tested at least in triplicate. Cultures were diluted to 2.5x10^3 cells/ml in sterile RPMI 1640 (Sigma, St. Louis, MO) with 2% glucose, buffered with 0.165 M MOPS and adjusted to pH 7.0. Plates were incubated at 35°C for 24 and 48 h

with shaking. Optical density at 600 nm was read with a Biotek Synergy 2 microplate reader (Fisher Scientific, Waltham, MA); background due to medium was subtracted from all readings. The relative growth was calculated as the percentage of cell growth in drug containing medium relative to the cell growth in the absence of drug; the results were plotted as percent inhibition versus fluconazole concentration.

Construction of Plasmids. All primers used are listed in Table 2. An *ERG3* deletion construct for *C. parapsilosis* was generated by amplifying an *Apa*I-*Xho*I-containing fragment consisting of flanking regions upstream -280 to +51 relative to the start codon of *C. parapsilosis ERG3* using primers ERG3-A and ERG3-B, as well as a *Not*I-*Sac*II-containing fragment of downstream flanking regions +1047 to +1868 using primers ERG3-C and ERG3-D. These upstream and downstream fragments of *ERG3* were cloned upstream and downstream, respectively, of the *SAT1*-flipper cassette in plasmid pSFS2 to result in plasmid p77ERG3. Additionally, the coding region of *ERG3* was amplified from either the Isolate 1 or Isolate 2 with primers ERG3-A and ERG3-E. Each of these *Apa*I-*Xho*I-containing fragments replaced the upstream sequence in cassette p77ERG3 to introduce the entire gene, creating plasmids p77ERG3comp and p76ERG3.

Similarly, an *ERG3* deletion construct for *C. albicans* was generated by amplifying an *Apa*I-*Xho*I-containing fragment consisting of flanking regions upstream -350 to +39 relative to the start codon of *C. albicans ERG3* using primers CaERG3A-F and CaERG3B-R, as well as a *Not*I-*Sac*II-containing fragment consisting of flanking regions +997 to +1677 downstream of the start codon using primers CaERG3C-F and CaERG3D-R. These upstream and downstream fragments were cloned upstream and

downstream, respectively, of the SAT1-flipper cassette in plasmid pSFS2, resulting in pCaERG3M1.

Candida parapsilosis *Transformation. C. parapsilosis* strains were transformed by electroporation as described previously but with some modifications (31). Cells were grown for 6 hours in 2 mL YPD liquid medium and then 4 µL of this cell suspension was passed to 50 mL of fresh YPD liquid medium and grown overnight at 30°C in a shaking incubator. When the culture's optical density at 600 nm reached 2.0, cells were collected by centrifugation, resuspended in 1 mL 10x TE buffer, 1 mL lithium acetate, and 8 mL of deionized water, and then reincubated at 30°C for 1 hour. Freshly prepared 1M dithiothreitol was added to the cell suspension, and cells were incubated for an additional 30 minutes. Cells were then washed twice with ice-cold water and then once with ice-cold 1 mM sorbitol. Finally, the cells were resuspended in 100 µL of fresh ice-cold 1 mM sorbitol. The gel-purified *Apa*I-*Sac*I fragment from the appropriate plasmid was mixed with 40 µL of competent cells and transferred into a chilled 2-mm electroporation cuvette. The reaction was carried out at 1.5 kV, using a Celljject Pro Electroporator (Thermo). Immediately following, 1 mL of YPD containing 1 M sorbitol was added and the mixture was transferred to a 1.5 mL centrifuge tube. Cells were allowed to recover at 30°C for 6 hours. Finally, 100 µL was removed and plated to YPD agar plates containing 200 µg/mL nourseothricin and 1 M sorbitol. Transformants were selected after at least 48-hours growth at 30°C.

RNA Isolation and Sequencing. RNA was isolated using the hot phenol method of RNA isolation described previously (33). RNA concentrations were determined using a Nanodrop spectrophotometer (Nanodrop Products), and RNA integrity was verified

using a Bioanalyzer 2100 (Agilent Technologies). Barcoded libraries were prepared using the Lexogen mRNA Sense kit for Ion Torrent according to manufacturer's standard protocol. Libraries were sequenced on the Ion Torrent Proton sequencer. Individual sample fragments were concatenated to form the whole sample fastq file. Files were then run through FASTQC to check data quality. Any reads with a phread score <20 were trimmed. Reads were then aligned to the *C. parapsilosis* CDC317 reference transcriptome using RNA-Star long method. After alignment, transcriptome alignment counts were gathered. The read counts for each sample were normalized using transcripts per kilobase million (TPM) method. These data have been deposited in the Gene Expression Omnibus repository under the accession number GSE98986.

Southern Hybridization. Genomic DNA (gDNA) for use with Southern blotting was prepared as described previously (34), digested with appropriate restriction endonucleases, separated on a 1 % agarose gel, stained with ethidium bromide, and transferred by vacuum blotting to a nylon membrane. After UV crosslinking, membranes were probed and detected using the Amersham ECL Direct nucleic acid labeling and detection system according to the manufacturer's instructions.

Whole Genome Sequencing. Genomic DNA for library preparation was isolated using Qiagen Genomic-tip 100/G kit (Qiagen) following the manufacturer's Genomic DNA Preparation instructions. Paired-end DNA sequence libraries for Isolate 1 and for Isolate 2 were prepared and sequenced using the Ion Proton Torrent sequencer and aligned to the *C. parapsilosis* CDC317 reference genome sequence. The GATK Best Practices work flow was used, incorporating the following tools: bwa (193) v0.5.9 (aln and sample), Picard tools (http://picard.sourceforge.net) v1.107 (SortSam and

MarkDuplicates), samtools (194) v0.1.19 and GATK (195) v2.8. (RealignerTargetCreateor, IndelRealigner, BaseRecalibrator, PrintReads, ReduceReads, HaplotypeCaller). A population variants file for *C. parapsilosis* was downloaded from the Broad Institute website (https://www.broadinstitute.org/fungal-genome-initiative) and used as the –knownSites file in the GATK BaseRecalibrator step. The snpEff (196) v3.5 genetic variant annotation tool was used to annotate SNP and indel variants using the c_parapsilosis_CDC317 snpEff database. The GATK CombineVariants and SelectVariants tools were used to select SNPs found in Isolate 2 but not in Isolate 1 and SNPs that are heterozygous in Isolate 1 and homozygous in Isolate 2. The JBrowse Genome Browser (197) v1.11.6 was used to visualize sequence alignments at genomic positions in order to validate variant calls (35). Following installation of the *C. parapsilosis* CDC317 reference genome using the current chromosomal features file available at the Candida Genome Database (www.candidagenome.org), the whole genome sequencing (WGS) data for the parental Isolate 1 was uploaded and aligned to the reference chromosome map using Ymap (lovelace.cs.umn.edu/Ymap). WGS data for Isolate 2 was then installed utilizing Isolate 1 as the parental strain to allow for loss of heterozygosity (LOH) analysis (15). The NCBI accession number for these data is PRJNA361149.

Sequence Analysis of ERG3. The coding sequence of *ERG3* in *C. parapsilosis* was amplified by PCR from *C. parapsilosis* genomic DNA using the primers listed in Table 2, cloned into pCR-BLUNTII-TOPO using a Zero Blunt TOPO PCR cloning kit, and transferred into Escherichia coli TOP10 cells with selection on LB agar plates containing 50 µg/ml kanamycin. Plasmid DNA was purified (QIAquick PCR Purification

Kit, Qiagen) and sequenced on an ABI model 3130XL genetic analyzer using sequencing primers, resulting in a full-length sequence from both strands of *ERG3*. The sequencing was performed using a total of six sets of clones derived from three independent PCR reactions. The coding sequence of *ERG3* in Isolate 2 described in this study has been deposited in GenBank under accession number KT277771.

Sterol Analysis. Non-saponifiable lipids were extracted using alcoholic KOH. Samples were dried in a vacuum centrifuge (Heto) and were derivatized by the addition of 100 µl 90% BSTFA/ 10% TMS (Sigma), 200 µl anhydrous pyridine (Sigma) and heating for 2 hours at 80°C. TMS-derivitized sterols were analyzed and identified using GC/MS (Thermo 1300 GC coupled to a Thermo ISQ mass spectrometer, Thermo Scientific) with reference to retention times and fragmentation spectra for known standards. GC/MS data files were analyzed using Xcalibur software (Thermo Scientific) to determine sterol profiles for all isolates and for integrated peak areas (20).

Funding Information

The research contained in this manuscript was supported by National Institutes of Health (NIH) grant R01 AI058145 (P.D.R.). Partial support for DNA sequencing and analysis was provided by the Memphis Research Consortium (T.R.S.).

Acknowledgements

The authors thank Dr. Elizabeth L. Berkow for her contributions to the construction of the *C. parapsilosis ERG3* mutants used in this study, Dr. Joachim Morschhäuser for his invaluable expertise and for generously providing the pSFS2 plasmid used in gene disruption and complementation experiments, and Dr. Shirlean Goodwin for her assistance in the improvement of genomic DNA isolation and sequencing methods.

References

1. **Pfaller MA, Andes DR, Diekema DJ, Horn DL, Reboli AC, Rotstein C, Franks B, Azie NE.** 2014. Epidemiology and outcomes of invasive candidiasis due to non-albicans species of Candida in 2,496 patients: data from the Prospective Antifungal Therapy (PATH) registry 2004-2008. PLoS One **9:**e101510.
2. **Lockhart SR, Iqbal N, Cleveland AA, Farley MM, Harrison LH, Bolden CB, Baughman W, Stein B, Hollick R, Park BJ, Chiller T.** 2012. Species identification and antifungal susceptibility testing of Candida bloodstream isolates from population-based surveillance studies in two U.S. cities from 2008 to 2011. J Clin Microbiol **50:**3435-3442.
3. **Cleveland AA, Farley MM, Harrison LH, Stein B, Hollick R, Lockhart SR, Magill SS, Derado G, Park BJ, Chiller TM.** 2012. Changes in incidence and antifungal drug resistance in candidemia: results from population-based laboratory surveillance in Atlanta and Baltimore, 2008-2011. Clin Infect Dis **55:**1352-1361.
4. **Trofa D, Gacser A, Nosanchuk JD.** 2008. Candida parapsilosis, an emerging fungal pathogen. Clin Microbiol Rev **21:**606-625.
5. **Garcia-Effron G, Katiyar SK, Park S, Edlind TD, Perlin DS.** 2008. A naturally occurring proline-to-alanine amino acid change in Fks1p in Candida parapsilosis, Candida orthopsilosis, and Candida metapsilosis accounts for reduced echinocandin susceptibility. Antimicrob Agents Chemother **52:**2305-2312.
6. **Kabbara N, Lacroix C, Peffault de Latour R, Socie G, Ghannoum M, Ribaud P.** 2008. Breakthrough C. parapsilosis and C. guilliermondii blood stream infections in allogeneic hematopoietic stem cell transplant recipients receiving long-term caspofungin therapy. Haematologica **93:**639-640.
7. **Pfeiffer CD, Garcia-Effron G, Zaas AK, Perfect JR, Perlin DS, Alexander BD.** 2010. Breakthrough invasive candidiasis in patients on micafungin. J Clin Microbiol **48:**2373-2380.
8. **Pfaller MA, Rhomberg PR, Messer SA, Jones RN, Castanheira M.** 2015. Isavuconazole, micafungin, and 8 comparator antifungal agents' susceptibility profiles for common and uncommon opportunistic fungi collected in 2013: temporal analysis of antifungal drug resistance using CLSI species-specific clinical breakpoints and proposed epidemiological cutoff values. Diagn Microbiol Infect Dis **82:**303-313.

9. **Silva AP, Miranda IM, Guida A, Synnott J, Rocha R, Silva R, Amorim A, Pina-Vaz C, Butler G, Rodrigues AG.** 2011. Transcriptional profiling of azole-resistant Candida parapsilosis strains. Antimicrob Agents Chemother **55:**3546-3556.
10. **Grossman NT, Pham CD, Cleveland AA, Lockhart SR.** 2015. Molecular mechanisms of fluconazole resistance in Candida parapsilosis isolates from a U.S. surveillance system. Antimicrob Agents Chemother **59:**1030-1037.
11. **Branco J, Silva AP, Silva RM, Silva-Dias A, Pina-Vaz C, Butler G, Rodrigues AG, Miranda IM.** 2015. Fluconazole and Voriconazole Resistance in Candida parapsilosis Is Conferred by Gain-of-Function Mutations in MRR1 Transcription Factor Gene. Antimicrob Agents Chemother **59:**6629-6633.
12. **Berkow EL, Manigaba K, Parker JE, Barker KS, Kelly SL, Rogers PD.** 2015. Multidrug Transporters and Alterations in Sterol Biosynthesis Contribute to Azole Antifungal Resistance in Candida parapsilosis. Antimicrob Agents Chemother **59:**5942-5950.
13. **Moudgal V, Little T, Boikov D, Vazquez JA.** 2005. Multiechinocandin- and multiazole-resistant Candida parapsilosis isolates serially obtained during therapy for prosthetic valve endocarditis. Antimicrob Agents Chemother **49:**767-769.
14. **Znaidi S, Weber S, Al-Abdin OZ, Bomme P, Saidane S, Drouin S, Lemieux S, De Deken X, Robert F, Raymond M.** 2008. Genomewide location analysis of Candida albicans Upc2p, a regulator of sterol metabolism and azole drug resistance. Eukaryot Cell **7:**836-847.
15. **Abbey DA, Funt J, Lurie-Weinberger MN, Thompson DA, Regev A, Myers CL, Berman J.** 2014. YMAP: a pipeline for visualization of copy number variation and loss of heterozygosity in eukaryotic pathogens. Genome Med **6:**100.
16. **Prasad R, Rawal MK.** 2014. Efflux pump proteins in antifungal resistance. Front Pharmacol **5:**202.
17. **Denning DW.** 2003. Echinocandin antifungal drugs. Lancet **362:**1142-1151.
18. **Park S, Kelly R, Kahn JN, Robles J, Hsu MJ, Register E, Li W, Vyas V, Fan H, Abruzzo G, Flattery A, Gill C, Chrebet G, Parent SA, Kurtz M, Teppler H, Douglas CM, Perlin DS.** 2005. Specific substitutions in the echinocandin target Fks1p account for reduced susceptibility of rare laboratory and clinical Candida sp. isolates. Antimicrob Agents Chemother **49:**3264-3273.
19. **Cowen LE, Steinbach WJ.** 2008. Stress, drugs, and evolution: the role of cellular signaling in fungal drug resistance. Eukaryot Cell **7:**747-764.
20. **Kelly SL, Lamb DC, Corran AJ, Baldwin BC, Kelly DE.** 1995. Mode of action and resistance to azole antifungals associated with the formation of 14 alpha-methylergosta-8,24(28)-dien-3 beta,6 alpha-diol. Biochem Biophys Res Commun **207:**910-915.
21. **Sanglard D, Coste A, Ferrari S.** 2009. Antifungal drug resistance mechanisms in fungal pathogens from the perspective of transcriptional gene regulation. FEMS Yeast Res **9:**1029-1050.
22. **Martel CM, Parker JE, Bader O, Weig M, Gross U, Warrilow AG, Rolley N, Kelly DE, Kelly SL.** 2010. Identification and characterization of four azole-resistant erg3 mutants of Candida albicans. Antimicrob Agents Chemother **54:**4527-4533.
23. **Vale-Silva LA, Coste AT, Ischer F, Parker JE, Kelly SL, Pinto E, Sanglard D.** 2012. Azole resistance by loss of function of the sterol Delta(5),(6)-desaturase gene (ERG3) in Candida albicans does not necessarily decrease virulence. Antimicrob Agents Chemother **56:**1960-1968.
24. **Hull CM, Bader O, Parker JE, Weig M, Gross U, Warrilow AG, Kelly DE, Kelly SL.** 2012. Two clinical isolates of Candida glabrata exhibiting reduced sensitivity to amphotericin B both harbor mutations in ERG2. Antimicrob Agents Chemother **56:**6417-6421.
25. **Young LY, Hull CM, Heitman J.** 2003. Disruption of ergosterol biosynthesis confers resistance to amphotericin B in Candida lusitaniae. Antimicrob Agents Chemother **47:**2717-2724.

26. **Jensen RH, Astvad KM, Silva LV, Sanglard D, Jorgensen R, Nielsen KF, Mathiasen EG, Doroudian G, Perlin DS, Arendrup MC.** 2015. Stepwise emergence of azole, echinocandin and amphotericin B multidrug resistance in vivo in Candida albicans orchestrated by multiple genetic alterations. J Antimicrob Chemother **70:**2551-2555.
27. **Kelly SL, Lamb DC, Kelly DE, Manning NJ, Loeffler J, Hebart H, Schumacher U, Einsele H.** 1997. Resistance to fluconazole and cross-resistance to amphotericin B in Candida albicans from AIDS patients caused by defective sterol delta5,6-desaturation. FEBS Lett **400:**80-82.
28. **Chau AS, Gurnani M, Hawkinson R, Laverdiere M, Cacciapuoti A, McNicholas PM.** 2005. Inactivation of sterol Delta5,6-desaturase attenuates virulence in Candida albicans. Antimicrob Agents Chemother **49:**3646-3651.
29. **Miyazaki Y, Geber A, Miyazaki H, Falconer D, Parkinson T, Hitchcock C, Grimberg B, Nyswaner K, Bennett JE.** 1999. Cloning, sequencing, expression and allelic sequence diversity of ERG3 (C-5 sterol desaturase gene) in Candida albicans. Gene **236:**43-51.
30. **Branco J, Ola M, Silva RM, Fonseca E, Gomes NC, Martins-Cruz C, Silva AP, Silva-Dias A, Pina-Vaz C, Erraught C, Brennan L, Rodrigues AG, Butler G, Miranda IM.** 2017. Impact of ERG3 mutations and expression of ergosterol genes controlled by UPC2 and NDT80 in Candida parapsilosis azole resistance. Clin Microbiol Infect doi:10.1016/j.cmi.2017.02.002.
31. **Reuss O, Vik A, Kolter R, Morschhauser J.** 2004. The SAT1 flipper, an optimized tool for gene disruption in Candida albicans. Gene **341:**119-127.
32. **CLSI.** 2008. Reference Method for Broth Microdilution Antifungal Susceptibility Testing of Yeasts; Approved Standard. CLSI Document M27-A3. 3 rd ed., Vol. 28. Wayne, Pennsylvania,. Clinical and Laboratory Standards Institute (CLSI).
33. **Schmitt ME, Brown TA, Trumpower BL.** 1990. A rapid and simple method for preparation of RNA from Saccharomyces cerevisiae. Nucleic Acids Res **18:**3091-3092.
34. **Amberg DC, Burke DJ, Strathern JN.** 2006. Isolation of yeast genomic DNA for southern blot analysis. CSH Protoc **2006**.
35. **Skinner ME, Uzilov AV, Stein LD, Mungall CJ, Holmes IH.** 2009. JBrowse: a next-generation genome browser. Genome Res **19:**1630-1638.

530 **Table 1.** *C. parapsilosis* strains and isolates used in this study

Strain/Isolate (Name)	Strain Background	Relevant Genotype/Characteristics	Reference
C. parapsilosis			
35177 (Isolate 1)	N/A	Antifungal drug susceptible	13
35176 (Isolate 2)	N/A	Antifungal drug resistant	13
E77U7G3 (Isolate 1- *erg3Δ/Δ*)	Isolate 1	*erg3Δ::FRT/erg3Δ::FRT*	This study
76B2E19 (Isolate 2- *erg3Δ/Δ*)	Isolate 2	*erg3Δ::FRT/erg3Δ::FRT*	This study
76C1B4 (Isolate 2- *ERG3*$^{WT/WT}$)	76B2E19	*erg3Δ:: ERG3*^{WT} *-FRT/ erg3Δ::ERG3*^{WT}*-FRT*	This study
C. albicans			
SC5314	N/A	wild-type	-
ScERG3M4C (SC5314- *erg3Δ/Δ*)	SC5314	*erg3Δ::FRT/ erg3Δ::FRT*	This study
GP1 (BR1- *ERG3*$^{WT/WT}$)	BWP17	*his1Δ/Δ::HIS1 arg4Δ/Δ::ARG4 ura3Δ/Δ::IRO1-URA3*	This study
E3AL1 (BR2- *erg3Δ/Δ*)	BWP17	*erg3Δ::ARG4/erg3Δ:HIS1 ura3Δ/Δ::IRO1-URA3*	This study

531 **Table 2.** Primers used in this study

Primer	Sequence[a]
C. parapsilosis Gene Disruption/Complementation	
ERG3-A	5'-GACAAACAAAATAAGGGCCCAAAATTAAAGG-3'
ERG3-B	5'- AGCATATAGTCTCTCGAGTAGGTAATAAT-3'
ERG3-C	5'-GATAGCCGCGGAAGATCATACAGAAGAC-3'
ERG3-D	5'-AAAATAGAGCTCCTGGGTGGGAATTAT -3'
ERG3-E	5'-AAAATACAGTTACTCGAGGGGAATTAT-3'
C. parapsilosis ERG3 Sequencing	
ERG3-A	5'-CCCACGTTTATTTCACTAGATCC-3'
ERG3-B	5'-GGTTGCCTTGACCAACCC-3'
ERG3-C	5'-GGGAATGGGCAATAGGGACAC-3'
ERG3-D	5'-GGTTGCCTTGACCAACCC-3'
C. albicans Gene Disruption	
CaERG3A-F	5'- ATCTGATTTATATATGGGCCCAAGTGTTTG-3'
CaERG3B-R	5'-AAAAGATAATAGTCTCGAGTTTCTAGTACG-3'
CaERG3C-F	5'-ATAGCCGCGGTAACTCTTACAGAAGACC-3'
CaERG3D-R	5'-TGTGATGTGAGCTCGTTAGTATTATTTTCA-3'

532 a- Underlined sequences indicate introduced restriction sites.

533

534 **Table 3A.** Azole antifungal susceptibilities for *C. albicans* and *C. parapsilosis* isolates [a]

	Fluconazole				Voriconazole				Itraconazole				Posaconazole			
Isolate	24h		48h		24h		48h		24h		48h		24h		48h	
C. parapsilosis																
Isolate 1 [b]			1				0.03									
Isolate 2 [b]			**>64**				**>16**									
Isolate 1	0.25	0.25	0.25	0.5	≤0.03	≤0.03	0.06	≤0.03	≤0.03	≤0.03	≤0.03	0.06	≤0.03	≤0.03	≤0.03	≤0.03
Isolate 2	≤0.125	≤0.125	**>64**	**>64**	≤0.03	≤0.03	**>16**	**>16**	≤0.03	≤0.03	**>16**	**>16**	≤0.03	≤0.03	**>16**	**>16**
Isolate 1- *Δerg3*	≤0.125	≤0.125	**>64**	**>64**	≤0.03	≤0.03	**>16**	**>16**	≤0.03	≤0.03	**>16**	**>16**	≤0.03	≤0.03	**>16**	**>16**
Isolate 2- *Δerg3*	≤0.125	≤0.125	**>64**	**>64**	≤0.03	≤0.03	**>16**	**>16**	≤0.03	≤0.03	**>16**	**>16**	≤0.03	≤0.03	**>16**	**>16**
Isolate 2-*ERG3*$^{WT/WT}$	0.25	0.25	≤0.125	0.5	≤0.03	≤0.03	≤0.03	≤0.03	≤0.03	≤0.03	0.06	0.125	≤0.03	≤0.03	0.06	≤0.03
C. albicans																
SC5314	≤0.125	≤0.125	≤0.125	≤0.125	≤0.03	≤0.03	≤0.03	≤0.03	0.06	≤0.03	≤0.03	≤0.03	≤0.03	≤0.03	≤0.03	≤0.03
SC5314- *Δerg3*	**>64**	**>64**	**>64**	**>64**	**>16**	**>16**	**>16**	**>16**	**>16**	**>16**	**>16**	**>16**	**>16**	**>16**	**>16**	**>16**
BWP17	≤0.125	≤0.125	≤0.125	≤0.125	≤0.03	≤0.03	0.06	≤0.03	≤0.03	≤0.03	≤0.03	≤0.03	0.125	≤0.03	0.06	≤0.03
BWP17- *Δerg3*	**>64**	**>64**	**>64**	**>64**	**>16**	**>16**	**>16**	**>16**	**>16**	**>16**	**>16**	**>16**	**>16**	**>16**	**>16**	**>16**

535 a- All values are in μg/ml; values in bold are resistant.

536 b- MIC values as reported previously determined using the previous CLSI M27-A2 recommended methodologies (13).

537

538 **Table 3B.** Echinocandin and amphotericin B susceptibilities for *C. albicans* and *C.*

539 *parapsilosis* isolates [a]

Isolate	Anidulafungin			Caspofungin			Micafungin			Amphotericin B	
	24h		48h	24h		48h	24h		48h	24h	
C. parapsilosis											
Isolate 1 [b]	-	-	1	-	-	2	-	-	**8**	0.25	
Isolate 2 [b]	-	-	2	-	-	**>16**	-	-	**>16**	0.5	
Isolate 1	2	2	-	1	1	-	2	2	-	0.5	0.5
Isolate 2	**4**	**4**	-	2	1	-	**4**	**4**	-	0.5	0.5
Isolate 1- *Δerg3*	**4**	**4**	-	2	2	-	**8**	**8**	-	0.5	1
Isolate 2- *Δerg3*	**4**	**4**	-	2	2	-	**4**	**4**	-	0.5	0.5
Isolate 2-*ERG3*$^{WT/WT}$	2	2	-	1	0.5	-	2	2	-	0.25	0.5
C. albicans											
SC5314	≤0.015	≤0.015	-	0.25	0.25	-	0.03	0.03	-	0.25	0.5
SC5314- *Δerg3*	0.06	0.06	-	0.25	**0.5**	-	0.06	0.06	-	0.5	0.5
BWP17	≤0.015	≤0.015	-	0.25	0.25	-	0.03	0.03	-	0.25	0.5
BWP17- *Δerg3*	0.06	0.06	-	0.25	0.25	-	0.06	0.06	-	0.5	0.5

540 a- All values are in μg/ml; values in bold are non-susceptible according to CLSI clinical

541 breakpoints.

542 b- MIC values as reported previously determined using the previous CLSI M27-A2

543 recommended methodologies (13).

544

545 **Table 4.** Genes involved in sterol metabolic processes overrepresented among the
546 upregulated genes in Isolate 2 relative to Isolate 1.

Gene ID	*C. parapsilosis* Gene Name	*S. cerevisiae* Gene Name	*C. albicans* Gene Name	Fold Change Sample A	Fold Change Sample B
CPAR2_601530	-	*GRE2*	-	4.8	5.0
CPAR2_201490	-	-	-	7.2	1.7
CPAR2_405010	-	***ERG6***	***ERG6***	2.3	3.8
CPAR2_202280	-	*DAP1*	*DAP1*	3.3	1.6
CPAR2_405900	**-**	***ERG24***	***ERG24***	2.0	2.7
CPAR2_103490	-	*ATF2*	-	2.3	2.2
CPAR2_801560	-	*ERG27*	*ERG27*	2.2	2.2
CPAR2_303740	***ERG11***	***ERG11***	***ERG11***	1.6	2.6
CPAR2_801410	**-**	***ERG25***	***ERG25***	1.8	2.2
CPAR2_105000	-	*YEH1*	-	2.0	2.0
CPAR2_210480	-	***ERG1***	***ERG1***	1.7	2.2
CPAR2_207280	***UPC2***	***UPC2***	***UPC2***	1.8	1.8
CPAR2_703970	**-**	***ERG5***	***ERG5***	1.6	1.6
CPAR2_109890	**-**	***ERG2***	***ERG2***	1.6	1.5

547

548 Fold change values represents genes upregulated in Isolate 2 as compared to Isolate 1
549 a minimum of 1.5- fold in samples from independent experiments A and B. Genes
550 shown in bold have orthologs regulated by *CaUPC2*

551

552

553 **Table 5.** Sterol composition for each isolate and each *ERG3* mutant (shown as percent
554 of total sterols)

Sterol	Isolate 1	Isolate 2	Isolate 1 *erg3Δ/ erg3Δ*	Isolate 2 $ERG3^{WT}/ERG3^{WT}$
Ergosta-5,7,24(28)-tetranol	4.0	0.5	0.4	0.5
Unknown m/z 470	--	--	7.0	--
Zymosterol	4.2	7.5	--	1.9
Ergosterol	65.4	9.1	--	51.8
Ergosta-7,22-dienol	9.3	71.7	76.8	22.3
Fecosterol (E8, 24(28))	1.4	0.6	0.9	0.7
Ergosta-8-enol	--	0.8	1.2	0.6
Ergosta 5,7 dienol	6.3	0.4	0.3	8.6
Episterol (E7, 24(28))	3.2	3.3	4.2	3.2
Ergosta-7-enol	1.9	4.2	8.4	6.6
Lanosterol/obtusifoliol	2.8	0.5	0.3	2.7
4,4,-diemthyl cholesta-8,24-dienol	1.7	1.4	0.6	1.1

555

556

557

Figure 1. Fluconazole MIC growth curves. Isolates 1 and 2 and their related strains were grown for (A) 24 hours and (B) 48 hours in the presence of the indicated concentrations of fluconazole.

Figure 2. Schematic representation of RNA and whole genome sequencing data for Isolate 2 as compared to Isolate 1. Colored circle segments represent contig boundaries. The outer track represents RNA sequence data, such that the green lines indicate those genes which are overexpressed in Isolate 2 by at least 1.5-fold and red lines indicate those genes which are underexpressed at 0.5-fold or less, relative to Isolate 1. The inner track represents sequence variants which are found in Isolate 2 but not in Isolate 1 for the whole genome sequence data. Overexpressed genes of the ergosterol biosynthetic process are labeled with *S. cerevisiae* ortholog gene names.

Figure 3. Horizontal tracks represents the *C. parapsilosis* contig as labeled. The black line running horizonatally through each contig represents the the predicted local copy number, with the center set equal to two, and divergences up or down indicating increased or decreased copy number at that loci, respectively. A region of segmental tetraploidy is denoted with an asterisk. Gray vertical lines (A) represent local allelic variation with the darker gray indicating higher concentrations of heterozygosity. Red vertical lines (B) represent loss of heterozygosity relative to the parent isolate (Isolate 1), with darker red indicating a greater degree of change in heterozygosity.

A.

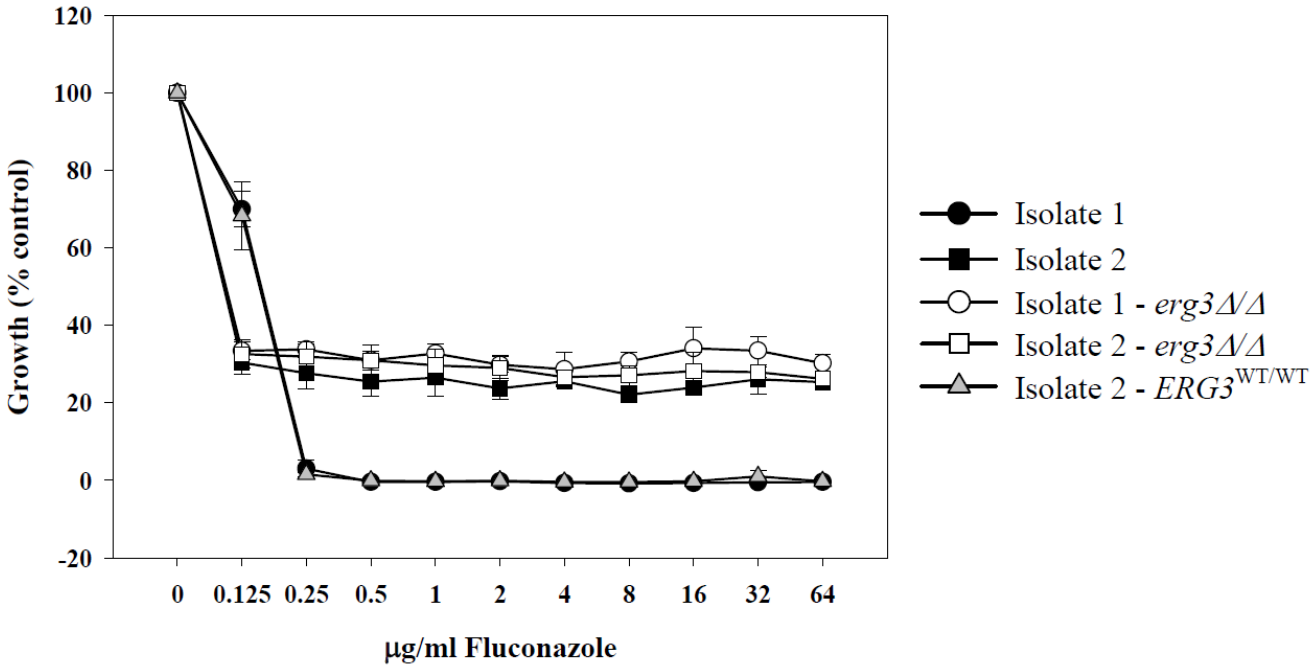

B.